ECS Journal of Solid State Science and Technology, **5** (3) P1-P7 (2016)
2162-8769/2016/5(3)/P1/7/$33.00 © The Electrochemical Society

Thermal Shields for Heat Loss Reduction in Siemens-Type CVD Reactors

A. Ramos,[z] J. Valdehita, J. C. Zamorano, and C. del Cañizo

Instituto de Energía Solar - Universidad Politécnica de Madrid, ETSI Telecomunicación, 28040 Madrid, Spain

The use of thermal shields to reduce radiation heat loss in Siemens-type CVD reactors is analyzed, both theoretically and experimentally. The potential savings from the use of the thermal shields is first explored using a radiation heat model that takes emissivity variations with wavelength into account, which is important for materials that do not behave as gray bodies. The theoretical calculations confirm that materials with lower surface emissivity lead to higher radiation savings. Assuming that radiation heat loss is responsible for around 50% of the total power consumption, a reduction of 32.9% and 15.5% is obtained if thermal shields with constant emissivities of 0.3 and 0.7 are considered, respectively. Experiments considering different thermal shields are conducted in a laboratory CVD reactor, confirming that the real materials do not behave as gray bodies, and proving that significant energy savings in the polysilicon deposition process are obtained. Using silicon as a thermal shield leads to energy savings of between 26.5–28.5%. For wavelength-dependent emissivities, the model shows that there are significant differences in radiation heat loss, of around 25%, when compared to that of constant emissivity. The results of the model highlight the importance of having reliable data on the emissivities within the relevant range of wavelengths, and at deposition temperatures, which remains a pending issue.

Manuscript submitted November 18, 2015; revised manuscript received December 18, 2015. Published 00 0, 2016.

Scope

90% of the polysilicon currently produced worldwide is demanded by the photovoltaic (PV) market, leaving the remaining amount for the microelectronics industry.[1,2] The chemical route -via chemical vapor deposition (CVD) of high purity trichlorosilane (TCS) on a hot filament, the so-called Siemens technology- currently dominates polysilicon production. High quality polysilicon is obtained, at the expense of high energy consumption.[3,4]

In the case of polysilicon for PV (also known as solar grade silicon) the process accounts for between a quarter and a third of the total energy consumption.[5–7] Thus, lowering the energy consumption of the Siemens process is essential to achieving the two wider objectives for silicon-based PV technology: low production cost and low energy payback time.

Furthermore, current price levels also press polysilicon producers to reduce their production costs even more if they are seeking a sustainable business.[8]

As radiation heat loss is the major contributor to energy consumption,[9] in this work the potential of thermal shields to reduce radiation heat loss in an industrial Siemens reactor is studied. Thermal (radiation) shields have been implemented in a number of CVD reactors; e.g. for layer deposition in superconducting devices or for the epitaxial growth of silicon layers.[10,11] Several proposals have recently been made for polysilicon production,[12–14] but to our knowledge quantitative analysis supported by experimental data has not been provided in any of them.

Radiation heat loss as regards thermal shields in a Siemens-type CVD reactor is studied first here using a theoretical model. Then, the theoretical results are compared with the experimental results in a laboratory Siemens reactor. Discussion of the latter will offer insights into the accuracy of theoretical calculations depending on the thermal shield materials' optical properties, highlighting the relevance of the variation in optical properties with the wavelength for thermal shield materials.

Potential to Reduce Radiation Heat Losses

First, the radiative heat transfer phenomenon is briefly described and the radiation heat loss model is presented. Then, theoretical radiation heat loss calculations for different thermal shields in an industrial Siemens reactor are put forward.

Radiative heat transfer.—Radiative heat transfer - also known as thermal radiation - describes the science of heat transfer caused by electromagnetic waves. These electromagnetic waves have the property of traveling through a vacuum or matter-containing media. The temperature of the radiant body governs the thermal radiation emission, and it occurs in the 0.1 to 100 μm wavelength range.[15,16] It is not the aim of this section to explain the thermal radiation phenomenon in detail, but to describe a number of concepts and properties of the radiation heat transfer mechanism that will support the arguments we develop in this document.

As regards the radiation properties, four dimensionless magnitudes are defined: absorptance (α), reflectance (ρ), transmittance (τ) and emissivity (ε). Absorptance, reflectance and transmittance are defined as the ratio of the total amount of radiation absorbed, reflected or transmitted by a surface to the total amount of radiation incident on the surface, respectively. The emissivity[a] Emissivity is defined as the ratio of the power per unit area radiated by a surface to the power per unit area radiated by a black body at the same temperature. These properties for real surfaces are dependent on temperature, direction and wavelength. The relationship indicated in Equation 1 is obtained by applying the energy balance to any real surface.

$$\alpha + \rho + \tau = 1 \qquad [1]$$

In addition, according to Kirchhoff's law, all opaque surfaces ($\tau = 0$) reach $\varepsilon_\lambda(\lambda, T) = \alpha_\lambda(\lambda, T)$.[15,16]

A black body is defined as any body that emits and absorbs the maximum possible radiation in all wavelengths, that is: $\alpha = 1,\ \rho = \tau = 0$. Plack's law defines the spectral radiated power of a black body. In addition, according to Stefan-Boltzmann's law the expression for the total radiation emitted per unit area of a black body is indicated in Equation 2; where T is the temperature and σ the Boltzmann constant.

$$E_b(T) = \sigma T^4 \qquad [2]$$

However, the majority of the surfaces do not behave as black bodies; thus, the gray body concept arises. A gray body is any opaque body ($\tau = 0,\ \alpha + \rho = 1$) whose reflectance, absorptance and emissivity properties are non dependent on the wavelength. The behavior of many real surfaces can be approximated to that of a gray body; in Equation 3 the expression of the total radiation emitted per unit area of a gray body is presented.

$$E_g(T) = \varepsilon_g \sigma T^4 \qquad [3]$$

The parameter ε_g corresponds to the emissivity of a gray body.

But, being more rigorous, real surfaces do not necessary behave as gray bodies, and their properties vary with the wavelength for a

[z]E-mail: alba.ramos@ies-def.upm.es

[a]Some authors refer to this parameter as 'emittance'. In this work emissivity and emittance are the same concept; however, there is a subtle difference between the two.[16]

given temperature. These surfaces radiate a different fraction ε_λ at each wavelength; thus, the expression of the total radiation emitted per unit area of a real surface is indicated in Equation 4. Note that the parameter ε_r in Equation 4 is calculated by means of Equation 5; that is, integrating ε_λ along all the radiation spectrum.

$$E_{real}(T) \cong \varepsilon_r \sigma T^4 \quad [4]$$

$$\varepsilon_r = \frac{\int_0^\infty \varepsilon_\lambda E_{b\lambda}\, d\lambda}{\int_0^\infty E_{b\lambda}\, d\lambda} \quad [5]$$

Real material properties.—As said previously, the radiative properties of real materials are not necessarily those of gray bodies. The difficulty is how to characterize the radiative properties of a selected material under working conditions. The reflectance (ρ_λ) and transmittance (τ_λ) of real surfaces can be determined by means of the Fourier transform infrared spectroscopy (FTIR);[17] thus, from Equation 1 absorptivity (α_λ) can be obtained. But these measurements are typically performed at room temperature; there are no overall techniques for the measurement of radiative properties at high temperatures. It is true that for certain materials, in particular for some metals, it is acceptable to consider that their radiative properties remain constant with temperature, although this cannot be easily generalized.[16,18,19]

Radiation heat loss model.—A radiation heat loss model for heat loss calculations in a Siemens-type reactor was presented and described in detail in Ref. 20, and validated in Ref. 21. It is further developed within the framework of this research to broaden its applicability and account for materials that do not behave as gray bodies.

One parameter needs to be defined for radiation heat loss calculations: radiosity (J), the rate of outgoing radiant heat per unit area from a surface. It is the sum of the directly emitted heat flux (E) and the reflected incoming radiant heat flux from the surface (G). The fraction of heat flux from one surface to another is determined by the so-called configuration factor, or geometrical factor. The calculation of the configuration factors (F_{i-j}) is made using a geometric Hottel's crossed-string method.[22] In the present case note that the rods and the reactor wall have a cylindrical geometry.

If the material properties, the geometrical arrangement, the surface temperatures and the incoming and directly emitted radiant heat flux are known, the net heat flux exchanged (Q) in Watts from any surface (S_i), is obtained from the difference between the radiosity and the incoming radiant heat flux. Then, the net radiation heat flux exchanged for a certain surface i can be expressed as shown in Equation 6.

$$Q_i = S_i \cdot (J_i - G_i) = S_i \cdot J_i - \sum_{j=1}^{n} S_j \cdot F_{j-i} \cdot J_j \quad [6]$$

For a Siemens reactor of n-1 rods, a n-equations system needs to be solved, as the reactor wall is considered as an additional surface. The radiosities of each surface (Ji) are the unknowns of the system. The temperature of the rod surfaces and the reactor wall is known, as is the corresponding surface emissivities. Once the J_i is obtained for the n surfaces, the incoming radiant heat flux per unit area (G_i) is also known. Thus, the net radiation heat exchanged by each surface (Q_i) is obtained by substituting J_i and G_i in Equation 6.

To account for emissivity variations with the wavelength, radiation heat loss is obtained by means of Equations 7, 8, 9 and 10, which are solved independently for each wavelength

$$S_i \cdot \frac{1}{1-\varepsilon_i(\lambda)} \cdot J_i(\lambda) - \sum_{j=1}^{n} S_i \cdot F_{i-j} \cdot J_j(\lambda) = S_i \cdot \frac{\varepsilon_i(\lambda)}{1-\varepsilon_i(\lambda)} \cdot \sigma \cdot T_i^4 \quad [7]$$

$$E_i(\lambda) = \varepsilon_i(\lambda) \cdot \sigma \cdot T_i^4 \quad [8]$$

$$G_i(\lambda) = \frac{1}{1-\varepsilon_i(\lambda)} \cdot (J_i(\lambda) - E_i(\lambda)) \quad [9]$$

$$Q_i(\lambda) = S_i \cdot (J_i(\lambda) - G_i(\lambda)) \quad [10]$$

where $i = 1, ..., n$.

The net heat flux exchanged (Q_i) in Watts by any surface (S_i), is obtained by integrating $Q_i(\lambda)$ along all the radiation spectrum. In Equation 11 the net heat flux exchanged by a surface is presented; $E_b(\lambda)$ is the total radiation emitted per unit area of a black body indicated in Equation 2.

$$Q_i = \frac{\int_0^\infty Q_i(\lambda) E_b(\lambda)\, d\lambda}{\int_0^\infty E_b(\lambda)\, d\lambda} \quad [11]$$

This radiative model allows extra surfaces in the Siemens reactor to be considered and their positive or negative effect on heat savings studied. This can be the case of a thermal shield. A thermal shield is a cylinder surrounding the polysilicon rods and placed between them and the reactor wall. The presence of this shield may block a significant part of the radiated heat that otherwise would be lost through the reactor wall.

Now, the net heat flux exchanged (Q_i) in Watts by any surface (S_i), is again obtained by integrating $Q_i(\lambda)$ along all the radiation spectrum; but by replacing Equation 7 with Equations 12-15 (where $i = 1, ..., m-1$, and m is the number of thermal shields considered).

$$S_i \cdot \frac{1}{1-\varepsilon_i(\lambda)} \cdot J_i(\lambda) - \sum_{j=1}^{m} S_i \cdot F_{i-j} \cdot J_j(\lambda) = S_i \cdot \frac{\varepsilon_i(\lambda)}{1-\varepsilon_i(\lambda)} \cdot \sigma \cdot T_i^4 \quad [12]$$

$$S_m \cdot \frac{1}{1-\varepsilon_m(\lambda)} \cdot J_m(\lambda) - \sum_{j=1}^{m} S_m \cdot F_{m-j} \cdot J_j(\lambda) = S_m \cdot \frac{\varepsilon_m(\lambda)}{1-\varepsilon_m(\lambda)} \cdot \sigma \cdot T_m^4 \quad [13]$$

$$\left(S_m \cdot \frac{\varepsilon_s(\lambda)}{1-\varepsilon_s(\lambda)} + \frac{1}{\gamma(\lambda)}\right) \cdot \sigma T_m^4 - S_m \cdot \frac{\varepsilon_s(\lambda)}{1-\varepsilon_s(\lambda)} \cdot J_m(\lambda) = \frac{\sigma T_n^4}{\gamma(\lambda)} \quad [14]$$

$$\gamma(\lambda) = \frac{1}{S_m \cdot \varepsilon_s(\lambda)} + \frac{1}{S_n} \cdot \left(\frac{1}{\varepsilon_n(\lambda)} - 1\right) + \left(\frac{2}{\varepsilon_s(\lambda)} - 1\right) \cdot \sum_{i=m+1}^{n-1} \frac{1}{S_i} \quad [15]$$

Note that even if the emissivity values now considered may be wavelength dependent, materials still are considered opaque ($\tau = 0$).

Theoretical calculations.—The potential of different thermal shields for radiation heat savings in an industrial Siemens reactor is studied here. The equations presented above are applied to a 36-rod, state-of-the-art Siemens reactor, and as a first approach, the emissivity of the materials is considered constant and wavelength independent. The initial and final diameter of the polysilicon rods is 0.7 and 13 cm, respectively, and their length is 2 m.

In Figure 1 the heat loss due to radiation in Watts (W) throughout a polysilicon deposition process for a constant surface temperature of 1150°C is shown; the curves correspond to the case with no thermal shield and four cases with thermal shields. The emissivities of the thermal shields are 0.3, 0.45, 0.55 and 0.7. In Table I the theoretical radiation heat loss savings for the aforementioned thermal shields are presented. The radiation heat loss savings, compared to the heat loss if no thermal shield is considered, are 65.8, 52.6, 44.3 and 30.5% for thermal shield emissivities (ε) of 0.3, 0.45, 0.55 and 0.7, respectively. This means, assuming that the radiation heat loss is responsible for around 50% of the total power consumption, that with a thermal shield with $\varepsilon = 0.3$ a reduction in power consumption of 32.9% is obtained, while for $\varepsilon = 0.7$ the reduction would be of 15.5%.

The temperature reached by the different thermal shields depending on their emissivity is presented in Figure 2. In all cases, and from the beginning of the process, these temperatures are above 850°C, which will result in polysilicon deposition on these surfaces. Thus,

Table I. Theoretical radiation heat loss savings for different thermal shields.

Thermal shield ε [-]	Radiation heat loss savings [%]
0.3	65.8
0.45	52.6
0.55	44.3
0.7	30.5

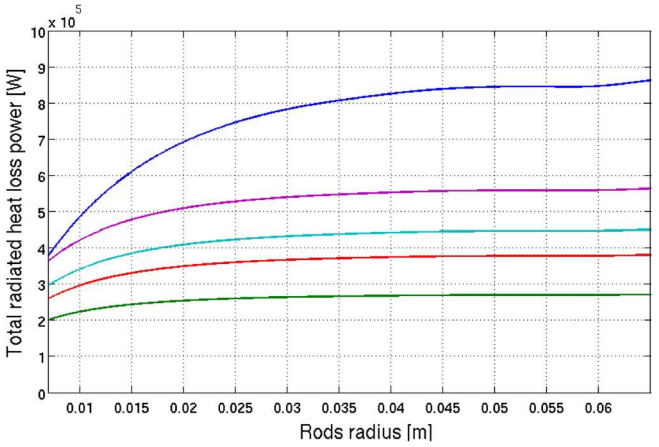

Figure 1. Radiation heat loss for a 36-rod Siemens reactor considering different thermal shields. No thermal shield (blue), ε = 0.7 (purple), ε = 0.55 (cyan), ε = 0.45 (red), ε = 0.3 (green).

after a few minutes into the deposition process the thermal shield's surface emissivity will be 0.7, that of silicon at high temperatures.[23] Furthermore, contamination issues can arise unless the shields are of a highly pure material. One way to overcome these drawbacks would be to use a thermal shield made of purified silicon.[12] Not only will it avoid contamination, but one can also collect the silicon deposited on the shields, adding it to the silicon produced in a batch.

The potential of thermal shields can be compared to the use of a polished or a reflective-coated inner wall of a reactor, which will lower the wall emissivity. For a given growth rate, and knowing the power consumption throughout a deposition process, and the initial and the final diameters of the polysilicon rods, the energy consumption in kWh/kg can be calculated. In Figure 3 the kWh/kg ratio for the case of a reflective-coated wall is compared to those considering a silicon thermal shield, no thermal shield and a thermal shield of ε = 0.3. For the calculations in Figure 3 the emissivity of the wall and the thermal

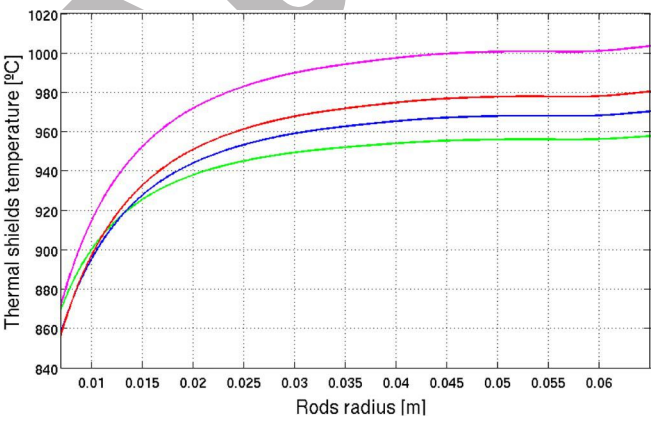

Figure 2. The temperature of thermal shields depending on their emissivity (ε) throughout a deposition process. Thermal shield emissivities: ε = 0.7 (purple), ε = 0.55 (red), ε = 0.45 (blue), ε = 0.3 (green).

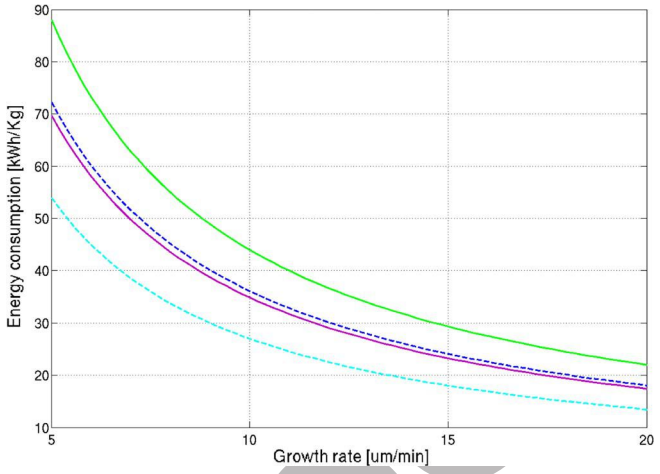

Figure 3. Total power consumption of a 36-rod Siemens reactor for different growth rates considering: no thermal shield -ε_{wall} = 0.5- (green), silicon thermal shield -ε = 0.7- (purple), thermal shield with ε = 0.3 (cyan) and no thermal shield and polished reactor wall -ε_{wall} = 0.3- (blue).

shields is considered constant throughout a deposition process; and the radiation heat loss is 50% of the total power consumption. The lowest kWh/kg ratio is obtained for a low emissivity thermal shield, and the kWh/kg ratio for that with a silicon thermal shield and a polished inner wall are quite close. However, note that the low emissivity thermal shield and the polished walls will not maintain their initial emissivities for more than a short period of time, as silicon or a silane-based compound will deposit. After a few minutes into the deposition process the blue curve will start to move slowly upwards until it reaches the green curve; and the cyan curve will quickly move to behave like the purple curve. Thus, the effect of a thermal shield is more efficient in terms of energy savings than considering a polished reactor wall; this statement is true even when considering a high initial emissivity value for the thermal shield (e.g., ε = 0.7).

Laboratory Scale Experiments

A number of experiments considering thermal shields are conducted in a laboratory Siemens reactor,[24] and the effect on radiation heat savings obtained is put forward.

Since the temperature of the thermal shield in the laboratory reactor will be lower than in the industrial case, the laboratory prototype allows us to test the effect of thermal shields with different emissivities. The key parameter for the selection of the thermal shield material is the emissivity (ε); but also, the material selected must be easily machinable, and available with the geometries and thickness required for its assembly inside the reactor chamber, so its mechanical strength must be assured. The following materials are evaluated: molybdenum, boron nitride, stainless steel, aluminum oxide (alumina), zirconium, graphite foil and silicon. Some of the relevant properties of these materials are presented in Table II; the values shown are considered wavelength independent since this dependence is unknown.

Table II. Properties of different materials considered for the thermal shields.[25,26]

Material	ε [-] (T = 25°C)	ε [-] (T ∼ 600°C)	Ease of machining
Molybdenum	-	0.8-0.9	Medium
Stainless steel	0.6-0.8	0.7-0.9	Low
Alumina	-	0.3-0.4	Medium
Boron nitride	0.9-0.95	-	Medium
Zirconium	-	0.1-0.3	High
Graphite foil	0.7-0.9	0.4-0.6	Low
Silicon	-	0.7	Medium

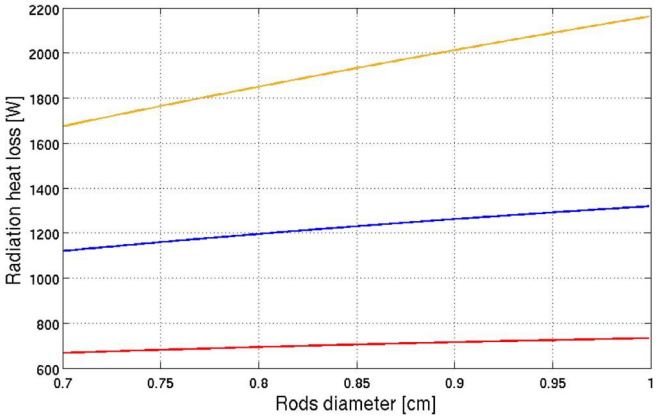

Figure 4. Radiation heat loss in the laboratory Siemens reactor for a 7-rod configuration considering a silicon thermal shield (blue), a low emissivity thermal shield -ε = 0.3- (red) and without thermal shield (orange).

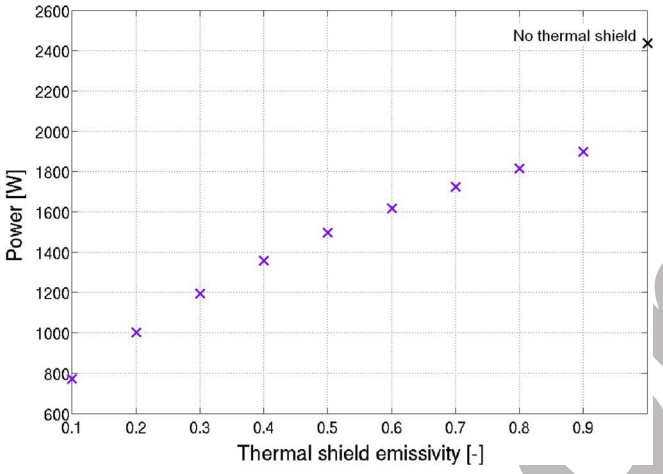

Figure 5. Laboratory Siemens reactor power consumption (P) predicted in theory for different thermal shield emissivities and for the case of no thermal shield considering a 7-rod configuration.

First, the radiation heat loss equations with thermal shields are applied to the laboratory Siemens reactor. The radiation heat loss for a 7-rod configuration with a low emissivity shield, with a silicon thermal shield and without thermal shield is presented in Figure 4; it can be seen how the lowest radiation heat losses are obtained for a low emissivity thermal shield. The temperatures reached by the thermal shields are in the range of 600-750°C.

The power consumption predicted by the model for different thermal shield emissivities and for that of no thermal shield, are presented in Figure 5. For these calculations a constant deposition temperature of 1100°C, the same growth rate and the same duration of the deposition processes, is considered, thus averaging the measured data. It can be seen that the lower emissivity of the thermal shield, the higher radiation heat savings.

Experiments with thermal shields.— A 7-rod configuration is chosen as a compromise solution between a dense compactness - a large number of rods - and the size of the reactor chamber. The length of the rods is 10 cm and their initial diameter is around 0.7 cm.

From the thermal shield materials listed in Table II, the following have been selected for testing: silicon, alumina and stainless steel. Different thickness of the selected materials are considered, and in some cases the outer surface of the thermal shields is silver coated[b].

[b]The silver coatings deposited are a few hundred nanometers thick.

Table III. Experiments conducted with 7-rod configuration in the laboratory Siemens reactor.

Experiment name	Description
No shield (No)	Without any thermal shield
Silicon shield (Si1)	Multi-crystalline silicon thermal shield (290 μm/layer; 3 layers)
Silicon shield (Si2)	Mono + Multi-crystalline silicon thermal shield (400 + 290 μm; 1 + 1 layers)
Silicon shield (Si3)	Mono + Multi-crystalline silicon thermal shield (400 + 290 × 4 μm; 1 + 4 layers)
Alumina shield (Alu1)	Alumina shield (1 mm thick)
Alumina shield (Alu2)	Alumina shield silver coated (1 mm thick)
Steel shield (Ste)	Stainless steel shield (1 mm thick)

Table IV. Experimental data obtained for the 7-rod configuration experiments: 'silicon shields'.

Experiment	(No)	(Si1)	(Si2)	(Si3)
$T_{deposition}$ [°C]	1106	1101	1108	1108
Si deposited [gr]	50.7	61.9	59.3	59.8
$Power_{average}$	2343	1979	2042	2122
Time [min]	392	406	385	375
T_{wall} [°C]	280	233	184	181
T_{shield} [°C]	-	678	641	616
Growth rate [μm/min]	2.9	3.5	3.6	3.6
Consumption [kWh/kg]	311	216	221	222
Energy savings [%]	-	28.4	26.8	26.5

The emissivity of silver is very low (ε ∼ 0.02-0.05), so if this coating withstands the process temperatures, it will act as a mirror making a non-opaque body behave almost as if it were.

The relevant data related to these experiments is presented in the following tables. First, the different thermal shields are described and related to their corresponding label in Table III. Then, the experimental results are grouped together in 'silicon shields' and 'alumina and stainless steel shields'; Tables IV and V, respectively.

From the data presented in Table IV, the energy savings obtained with the different silicon thermal shields are similar. The reduction in the kWh/kg ratio obtained considering thermal shields related to experiment (No) are between 26.5 and 28.4%. All these experiments were conducted under similar conditions and their duration is similar. Despite the fact that the deposition surface temperature is in all cases around 1100°C, there is a difference in the growth rate obtained in experiment (No). This is so because the presence of a thermal shield changes the distribution of the gas temperature, and higher temperatures are achieved in the gas surrounding the silicon rods.

From the data presented in Table V, the energy savings in kWh/kg, compared with experiment (No), vary between 15.1 and 30.7%. The

Table V. Experimental data obtained for the 7-rod configuration experiments: 'alumina and stainless steel shields'.

Experiment	(No)	(Alu1)	(Alu2)	(Ste)
$T_{deposition}$ [°C]	1106	1107	1108	1098
Si deposited [gr]	50.7	65.3	53.7	49.3
$Power_{average}$	2343	2333	1669	1915
Time [min]	392	430	404	388
T_{wall} [°C]	280	142	175	152
T_{shield} [°C]	-	736	705	570
Growth rate [μm/min]	2.9	3.6	3.2	3.0
Consumption [kWh/kg]	311	256	205	251
Energy savings [%]	-	15.1	30.7	16.8

kWh/kg values in the laboratory scale reactor are several times higher than those found in industrial processes, mainly since the process pressure is 6-7 times lower. Comparing experiments (Alu1) and (Alu2), the silver coating seems to be effective; however its behavior differs from that expected from its theoretical ε (further explanations will be presented in Discussion on energy savings section).

Lastly, in experiments conducted with silicon thermal shields etching is detected on the surface of the shields. This is attributed to the presence of $SiCl_4$ as a by-product of the reduction reaction. The occurrence of this phenomenon versus polysilicon deposition depends on the mol fraction of $SiCl_4$, which will depend on the deposition surface temperature.[27,28] High $SiCl_4$ concentrations and low temperatures favor the etching. However, as already explained, under industrial deposition conditions the temperature of the thermal shields will be such that polysilicon will be deposited on the thermal shields, and no etching is expected.

Discussion on energy savings.—From the above, energy savings have been confirmed for the 7-rod configuration experiments considering different thermal shields.

If the experimental data from Tables IV and V (average power consumption and energy savings) is compared with the theoretical calculations for different thermal shields (Figure 5), a good agreement for the case of no thermal shields is obtained; differences between both values are under 3.8%. Note that our calculations consider constant deposition conditions, while the experimental conditions of the deposition process vary slightly from one experiment to another.

For the experiments conducted with thermal shields, the averaged power consumption and energy savings obtained vary between 1667-2333 W and 15.1–30.7%, respectively. According to data presented in Figure 5, the previous values correspond to thermal shield emissivities above 0.6. In the case of the silicon thermal shields, the energy savings obtained correspond to $\varepsilon = 0.7$–0.8, for the alumina shields to $\varepsilon > 0.9$, for the silver coated alumina shield to $\varepsilon = 0.6$–0.7; and for the stainless steel shield to $\varepsilon > 0.9$. These ε values do not correspond to those found in the bibliography assuming the gray body approach, which is no surprise since the gray body approach simplifies much of the radiative behavior of real bodies.

Reflectance, transmittance and emissivity measurements.—With the aim of clarifying the real emissivity of the thermal shield materials tested in the laboratory Siemens reactor, reflectance (ρ) and transmittance (τ) measurements for different λ are taken. Both, ρ(λ) and τ(λ), can be measured directionally or integrated; in the present case integrated measurements are suitable since the materials considered do not have specular surfaces. These measurements are conducted at room temperature.

In Figure 6 the integrated transmittance measurements, within the wavelength range $\lambda \in (2.5$–$20)$ μm, for different thermal shields are presented. In all cases, noticeably for the silicon shield, the integrated transmittance is $\tau \neq 0$. Measurements for a silicon, alumina and stainless steel thermal shields are presented in Figure 6. The integrated transmittance measured is on average 41.3, 8.1 and 0.5% for the

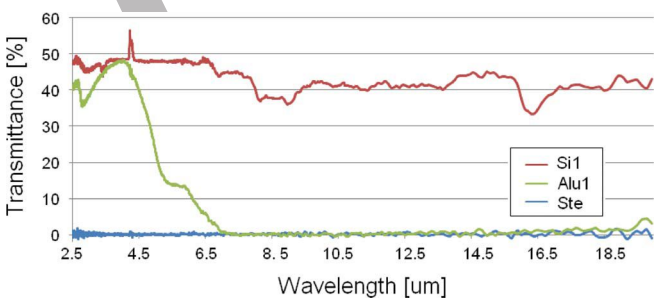

Figure 6. Integrated transmittance (τ) of: 290 μm multi-crystalline silicon (red), 1 mm alumina (green) and 1 mm stainless steel (cyan).

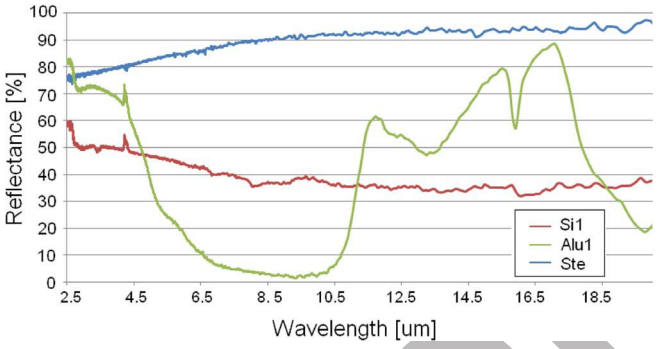

Figure 7. Integrated reflectance (ρ) of: 290 μm multi-crystalline silicon (red), 1 mm alumina (green) and 1 mm stainless steel (cyan).

290 μm multi-crystalline, 1 mm alumina and 1 mm stainless steel samples, respectively.

Integrated reflectance measurements are also conducted; ρ(λ) for $\lambda \in (2.5$–$20)$ μm for silicon, alumina and stainless steel are presented in Figure 7. From Figure 7, the averaged reflectance of the silicon sample is 40%, while the respective values for that of alumina and the stainless steel samples are 48.1 and 92.8%, respectively.

From the average values of the aforementioned transmittance and reflectance integrated measurements, only the stainless steel sample presents a very low transmittance. Materials experimentally tested in the laboratory Siemens reactor at room temperature definitely do not behave as gray bodies, and similar behavior can be expected at higher temperatures.[18,19] The latter explains the differences between the predicted energy savings and the empirically obtained ones. The next section discusses the effect that the wavelength-dependent emissivities can have on the radiation heat losses.

Discussion on the Contribution to the Radiation Heat Loss Model

The model for radiation heat loss is applied here for the radiation heat loss calculations of a 36-rod industrial Siemens reactor, considering thermal shields that do not behave as gray bodies. Two hypothetical thermal shields with an averaged $\varepsilon(\lambda) = 0.7$ are considered, with an emissivity variation presented in Figure 8. It can be seen that ε(λ) of material 1 is approximately constant, while ε(λ) of material 2 is heavily dependent on the wavelength.

The radiation heat loss for $\lambda \in (0.1, 20)$ μm, calculated for a 36-rod industrial Siemens reactor, is presented in Figure 9. The two scenarios presented; hereinafter scenarios 1 and 2, correspond to material 1 and material 2 thermal shields, respectively. In both cases, the radiation

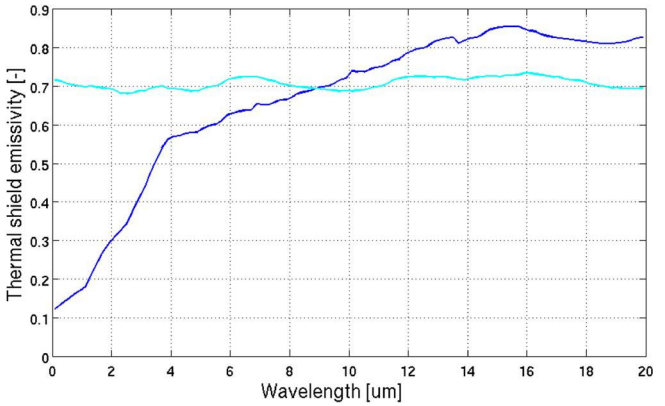

Figure 8. Emissivity ε(λ) for two different thermal shield materials: material 1 (cyan) and material 2 (blue). In both cases, the averaged $\varepsilon(\lambda) = 0.7$.

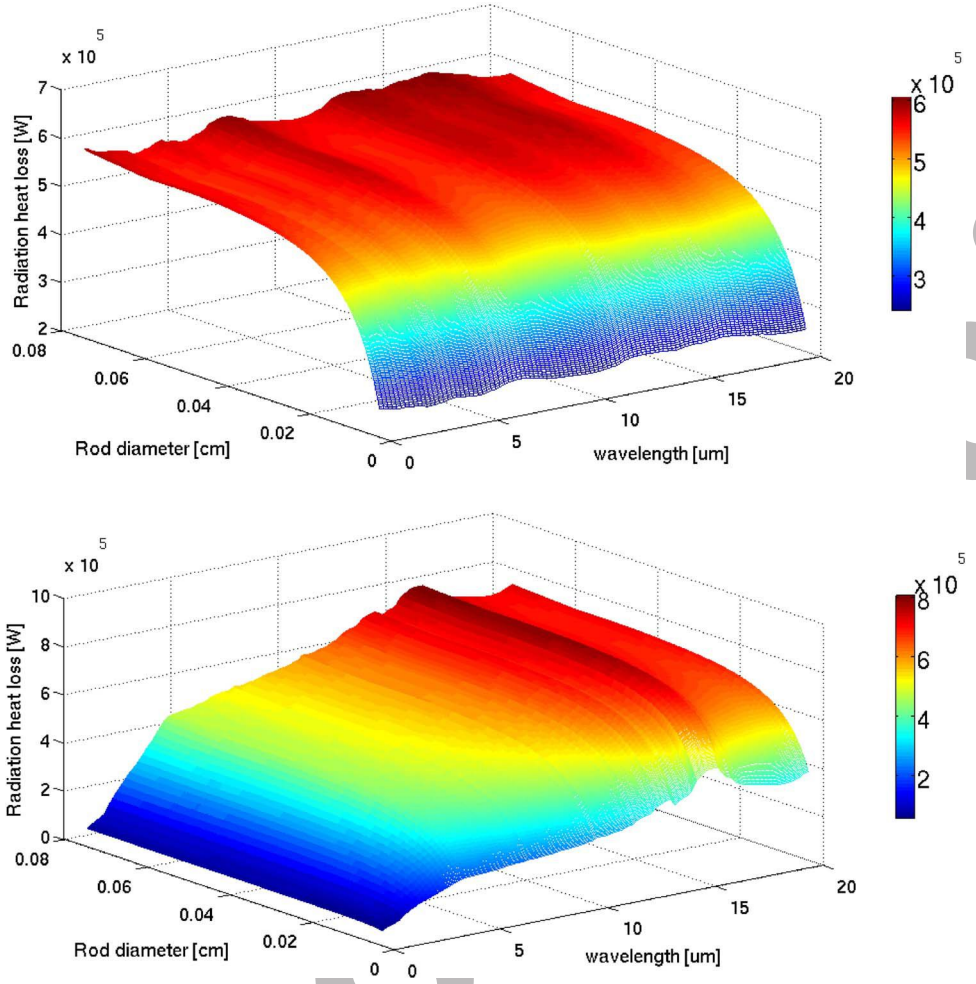

Figure 9. Radiation heat loss for different wavelengths for two different thermal shield materials: material 1 (top) and material 2 (bottom).

heat loss variation with λ is similar to the corresponding variation in $\varepsilon(\lambda)$ of the shield material considered.

When the surfaces presented in Figure 9 are integrated along the entire radiation spectrum, the radiation heat loss values presented in Figure 10 for scenarios 1 and 2 are obtained. This curves are presented together with the corresponding curve if a constant emissivity for the thermal shield $\varepsilon(\lambda) = 0.7$ is considered - scenario 3. It can be appreciated how the scenarios 1 and 3 are quite close, but great differences in radiation heat loss are obtained between scenarios 1 and 3, and scenario 2; the averaged differences are above 25%. As regards the thermal shield temperature, results obtained for scenarios 1 and 3 are also quite close; the temperature of the shields is around 870°C at the beginning of the deposition process, increasing rapidly until it reaches around 1000°C at the end of the process. In scenario 2, the thermal shield temperature has a similar behavior with temperature values that go from 860 to 975°C.

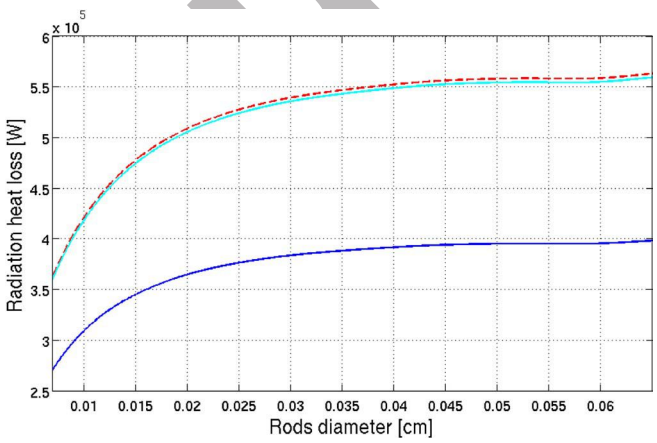

Figure 10. Radiation heat loss for different thermal shield materials: material 1 (cyan), material 2 (blue), obtained by integrating Figure 9 along all the radiation spectrum. The case of a material with a constant $\varepsilon(\lambda) = 0.7$ is presented for comparison (red).

The aforementioned differences above are explained since not all wavelengths contribute to the same extent to the radiation heat loss; in particular for these three scenarios, the greatest contribution of $\varepsilon(\lambda)$ occurs in the range $\lambda \in (1–6)\ \mu$m.

These results highlight the importance of having reliable data on the emissivities in the relevant range of wavelengths, and for the application of silicon CVD, at deposition process temperatures, which remains pending.

Conclusion

A radiation model for heat loss calculations in a Siemens-type reactor has been presented, in which the fraction of energy leaving a certain surface that arrives at another surface is evaluated using the geometric Hottel crossed-string method, and the effect of the emissivity variation with the wavelength is taken into account. A significant

potential for reducing radiation heat loss in Siemens reactors has been identified, considering different thermal shields. The model shows that materials with lower surface emissivities lead to higher radiation heat loss savings. The effect of a thermal shield is also more efficient in terms of energy savings than considering a polished reactor wall, even for a thermal shield with a high initial emissivity value.

Experiments considering different thermal shields are conducted in a laboratory Siemens reactor. It has been experimentally shown that significant energy savings in the polysilicon deposition process are obtained.

Silicon thermal shields have some advantages in terms of preventing contamination and collecting the silicon deposited on them, and energy savings of between 26.5-28.5% have been experimentally proven.

Reflectance and transmittance measurements as a function of wavelength are taken for the materials tested, proving that they do not behave as gray bodies at room temperature, and similar behavior can be expected at higher temperatures. Results highlight the importance of having reliable emissivity data on the materials involved at deposition temperatures, which remains pending.

Acknowledgments

The Spanish *Ministerio de Economía y Competitividad* is acknowledged for its support through the IPT 2012-0340-120000 project and *Comunidad de Madrid* through the MADRID-PV S2013/MAE-2780 project.

Ángel Morales, from the Centro de Investigaciones Energéticas Medioambientales y Tecnológicas (CIEMAT), Spain is acknowledged for his contribution to the reflectance and transmittance measurements.

References

1. K. Hesse, E. Schindlbeck, E. Dornberger, and M. Fischer, "Status and Development of Solar-Grade Silicon Feedstock," *24th European Photovoltaic Solar Energy Conference*, 883 (2009).
2. R. Berstein, "A shortage hits solar power," *The Wall Street Journal*, (2006).
3. A. F. B. Braga, S. P. Moreira, P. R. Zampieri, J. M. G. Bacchin, and P. R. Mei, "New processes for the silicon production of solar-grade polycrystalline silicon: A review," *Solar Energy Materials and Solar Cells*, **92**, 418 (2008).
4. C. Wang, T. Wang, P. Li, and Z. Wang, "Recycling of $SiCl_4$ in the manufacture of granular polysilicon in a fluidized bed reactor," *Chemical Engineering Journal*, **220**, (2013).
5. B. Ceccaroli and O. Lohne, *Handbook of Photovoltaic Science and Engineering, in: Solar Grade Silicon Feedstock*, 2nd Edition, pp. 169-217 (2011).
6. E. Alsema and M. de Wild-Scholten, "Reduction of the environmental impacts in crystalline silicon module manufacturing," *22nd European Photovoltaic Solar Energy Conference and Exhibition*, pp. 829-836, (2007).
7. S. Singer, "Photovoltaics: Getting Cheaper," *EcoQueen of Green*, (2007).
8. T. F. Ciszek, "Photovoltaic materials and crystal growth research and development in the gigawatt era," *Journal of Crystal Growth*, **393**, 2 (2014).
9. A. Ramos, A. Rodríguez, C. del Cañizo, J. Valdehita, J. C. Zamorano, and A. Luque, "Heat losses in a CVD reactor for polysilicon production: Comprehensive model and experimental validation," *Journal of Crystal Growth*, **402**, 138 (2014).
10. H. Griss, B. Caussat, H. Vergnes, and J. P. Couder, "An improvement in the behavior of LPCVD reactors: the dead zones reducers," *Chemical Vapor Deposition: Proceedings of the Fourteenth International and EUROCVD-11*, 194-201, 1997.
11. M. A. Gallivan, D. G. Goodwin, and R. M. Murray, "A Design Study for Thermal Control of a CVD Reactor for YBCO," *Proceedings of the 1998 IEEE International Conference on Control Applications*, Italy, 1998.
12. C. del Cañizo, G. del Coso, A. Luque, and J. C. Zamorano, "Thermal shield for silicon production reactors," [Pat.: WO 2012025513 A1], (2012).
13. G. Pazzaglia, M. Fumagalli, and M. Kulkarni, "Bell jar for siemens reactor including thermal radiation shield," [Pat.: WO 2011128729 A1], (2011).
14. J. Lee, J. Kim, S. Lee, and L. C. Winterton, "Chemical vapor deposition reactor having a radiant heat barrier layer for improving energy efficiency," [Pat.: WO 2011068283 A1], (2011).
15. F. Kreith and M. Bohn, *Heat transfer by radiation, Principles of heat transfer*, 6th Ed., Thomson, pp. 539-626, (2002).
16. M. F. Modest, *Radiative heat transfer*, 2nd Ed., Academic Press, 2003.
17. D. K. Schroder, *Semiconductor Material and Device Characterization*, 3rd Ed., Wiley-IEEE Press, 2006.
18. T. Paloposki and L. Liedquist, *Steel emissivity at high temperatures*, VTT Tiedotteita - Research Notes 2299, pp. 81, 2005.
19. C. E. Kennedy, *Review of Mid- to High- Temperature Solar Selective Absorber Materials*, National Renewable Energy Laboratory (NREL), 2002.
20. G. del Coso, C. Cañizo, and A. Luque, "Radiative energy loss in a polysilicon CVD reactor," *Solar Energy Materials & Solar Cells*, **95**, 1042 (2011).
21. A. Ramos, C. del Cañizo, J. Valdehita, J. C. Zamorano, and A. Luque, "Radiation heat savings in polysilicon production: Validation of results through a CVD laboratory prototype," *Journal of Crystal Growth*, **374**, 5 (2013).
22. R. Siegel and J. R. Howell, *Thermal radiation heat transfer*, McGraw-Hill, Siegel72, 1972.
23. G. del Coso, "Chemical decomposition of silanes for the production of solar grade silicon," Ph.D. Thesis, Universidad Politécnica de Madrid - ETSI Telecomunicación, 2010.
24. A. Ramos, C. del Cañizo, J. Valdehita, J. C. Zamorano, A. Rodríguez, and A. Luque, "Exploring polysilicon deposition conditions through a laboratory CVD prototype," *Physica Status Solidi C*, 10 (2012)
25. D. R. Lide (Ed.), *CRC Handbook of Chemistry and Physics*, National Institute of Standards and Technology, 2005.
26. G. G. Gubareff, J. E. Janssen, and R. H. Torborg, *Thermal Radiation Properties Survey*, Honeywell Research Center, 1960.
27. S. Grove, *Physics and Technology of Semiconductor Devices*, Willey, 1967.
28. S. M. Sze, *Semiconductor Devices: Physics and Technology*, 2nd Ed., Willey, 2001.